Proceedings of the 28th IEEE
EMBS Annual International Conference
New York City, USA, Aug 30-Sept 3, 2006

Partially Parallel MR Spectroscopic Imaging of Gliomas at 3T

Esin Ozturk[1, 2], Suchandrima Banerjee[1, 2], Sharmila Majumdar[1,2], Sarah J. Nelson[1,2]

Abstract— **Magnetic resonance spectroscopic imaging (MRSI) has been used to more accurately diagnose, localize, and assess progression and treatment response for gliomas. The main limitation of the MRSI is the long data acquisition times. A current approach is to reduce the amount of *k*-space data sampled by limiting the data acquisition to a central elliptical portion of *k*-space. This study investigated the feasibility of reducing the data acquisition time further for the MRSI data using two parallel imaging techniques and investigating the relative performance of sensitivity encoding (SENSE) and generalized autocalibrating partially parallel acquisitions (GRAPPA).**

I. Introduction

Brain cancer is a devastating disease with an estimated 18.820 new cases every year within the USA alone [1]. Gliomas are the most common type of brain tumors that originate from the glial cells, which are the support cells for neurons. The average survival time for high grade glioma patients is 12-15 months. Magnetic resonance imaging (MRI) techniques have been widely used in the diagnosis of gliomas.

Magnetic resonance spectroscopic imaging (MRSI) is an MRI technique that provides information about the brain chemistry. Magnetic spins of different metabolites resonate at different frequencies, due to the changes in their molecular environment, and their relative frequency difference to the frequency of tetra-methyl-silane (TMS) is used to form the parts per million (ppm) scale. Choline (Cho), creatine (Cr), and n-acetyl-aspartate (NAA) are the three most common metabolites observed in the brain tissue with long echo times (TE) that resonate at 3.2 ppm, 3.0 ppm, and 2.01 ppm respectively. An increase in the level of choline provides a marker for excessive cell growth or cell membrane turnover. The peak due to creatine and phosphocreatine reflects bioenergetics processes. NAA is the most abundant amino acid in brain that is synthesized in neurons, and is hypothesized to have a role in the removal of intracellular water from neurons. NAA levels have been observed to decrease in tumors. Lipid peaks which resonate at 1 ppm and doublet lactate peaks which resonate at 1.3 ppm are two other resonances that can be observed in the disease state. Lactate is a byproduct of anaerobic glycolysis, and is expected to be present in areas with poor oxygenation. Lipid may indicate cellular membrane breakdown due to necrosis, or may be due to aliasing from the skull and scalp outside of the small spectral FOV. The combination of 3D MRSI and MRI anatomical imaging has been suggested to result in better tumor localization, staging, and assessment of progression and treatment response than MR imaging alone [2].

Incorporating MRSI scans into patient protocols is desirable for the abundance of physiological information it provides, but the relatively long data acquisition time of MRSI has been challenging due to patient motion and discomfort. One solution to this problem has been to restrict the *k*-space data acquisition to a central elliptical portion [3]. This approach reduced the scan time from 37.5 minutes to 17.5 minutes with a repetition time (TR) of 1.1 s for a 16x16x8 array. Although the scan time has been reduced by 50% with this approach, it was still long for a patient to keep still. Recent availability of high field strengths (3T) and multi-channel head coils has resulted in higher signal intensities and variable coil sensitivities that add another dimension to the signal equation. In this study, we have investigated the feasibility of further reducing the MRSI scan time by sub-sampling elliptically acquired data, and reconstructing these spectra using sensitivity encoding (SENSE) and generalized autocalibrating partially parallel acquisitions (GRAPPA) based techniques.

II. Materials and Methods

A. Data Acquisition and Preparation

Spectroscopic imaging experiments were conducted on a uniform MRS phantom, 1 volunteer, and 5 glioma patients on a 3 T GE Signa EXCITE scanner (GE Healthcare, Milwaukee, WI) equipped with an eight channel RF coil (MRI Devices Inc, Gainesville, FL). Informed consent was obtained from the volunteer and patients prior to scanning. The MRS phantom contained major metabolites observed in the brain, which were Cho, Cr, NAA, and lactate. The imaging protocol included the acquisition of T1-weighted 3D SPGR (TR=26 ms, TE=3 ms, 3 mm slice thickness, 256x256 matrix, FOV=240x240 mm, flip angle = 40°), T2-weighted FLAIR (TR=10002 ms, TE=127 ms, TI=2200 ms, 3 mm slice thickness, 256x256 matrix, FOV=240x240 mm, flip angle=90°), and proton-density weighted fast gradient echo coil sensitivity images (TR=150 ms, TE=2.1 ms, 3 mm slice thickness, 64x64 matrix, FOV=300x300 mm, flip angle=20°). ^{1}H 3D MRSI data was acquired using PRESS volume localization with CHESS water suppression and VSS outer volume suppression. The spectral array

Manuscript received April 3, 2006. This research was funded by NIH grant P50 CA9729 and a grant jointly funded by the UC Discovery Program (LSIT 01-10107) and GE Healthcare. E. O. I., S. B., S. M., and S. J. N. Authors are with the [1]UCSF/UCB Joint Graduate Group in Bioengineering, University of California at San Francisco, San Francisco CA and University of California at Berkeley, Berkeley, CA, and [2]Department of Radiology, University of California at San Francisco, San Francisco, CA. (E. O. I. is the corresponding author. Phone: 415-514-4420; fax: 415-514-2550; e-mail: esin.ozturk@mrsc.ucsf.edu).

dimensions were 16x16x8 with 1 cm^3 nominal spatial resolution. The rectilinear *k*-space sampling was restricted to a central elliptical region in order to reduce the scan time to 17 min with TR=1.1s and TE=144 ms.

Spectroscopic data were sub-sampled to simulate a reduction factor (R) of two in k_x and k_y directions (R=4) for both SENSE and GRAPPA approaches. For the GRAPPA data, 2 full lines of data in k_x and another 2 lines in k_y were used as autocalibration (AC) lines. Figure 1 shows the sampled voxels in a given slice for elliptical, SENSE and GRAPPA methods. Black voxels represent the *k*-space data that are not sampled. The white lines in the GRAPPA sampling pattern represent the autocalibration lines. The original elliptical *k*-space sampling acquired 952 out of the full 2048 (16*16*8) voxels within 17:45 minutes with a TR=1.1s. SENSE elliptical datasets were composed of 238 acquired voxels that would result in 4:36 minutes of scan time. GRAPPA elliptical datasets had 582 acquired voxels that would take 10:67 minutes.

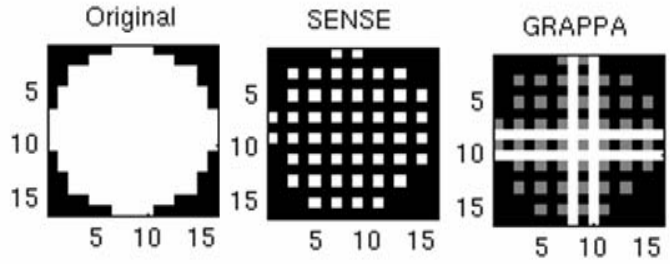

Fig. 1. The *k*-space sampling patterns for the elliptical, elliptical SENSE, and elliptical GRAPPA approaches.

B. Data Processing and Analysis

Regions of hyperintensity on FLAIR images were segmented using an in-house region growing algorithm to differentiate tumor areas (Tumor). Voxels in the PRESS box outside of the T2 hyperintensity were assumed to represent normal brain (Normal).

Individual proton density weighted images from the coils were divided by their combined sum of squares images. The resulting images were filtered with median and low-pass homomorphic filters consecutively to smooth the image discontinuities. Coil sensitivities were resampled to twice the spectral resolution for the in-plane directions. The images were dilated by a 3x3 kernel to preserve the edges of the image before resampling.

The spectral data for each coil were separately filtered by a 4 Hz Lorentzian filter, and Fourier transformed from *k*-space to the spatial domain and from time to frequency. After this pre-processing, each voxel was analyzed separately, and the spectra were phased, frequency shifted to match a template peak file, and water baseline was removed using in-house developed software [4]. The spectra from each channel were then combined as a weighted sum using the smoothed coil sensitivity maps.

SENSE reduced elliptical spectra were processed like the original elliptical spectra. The resultant spectral images had aliasing artifact due to their half FOV in both x and y directions. The spectra were unaliased by four fold using the SENSE algorithm [5] developed in Matlab 6.5 (The Mathworks Inc., Natick, MA) as,

$$v = (S^H \psi^{-1} S)^{-1} S^H \psi^{-1} A, \quad (1)$$

where S is the coil sensitivity values of the eight channels at the aliasing and original voxels, ψ is the noise receiver matrix, and A is the data measured by the eight coils, and v is the vector of unaliased original and aliasing voxels. Analysis of the effect of the SENSE algorithm on noise amplification was performed using the geometry factor that was calculated for each unfolded pixel, *i*, defined as follows:

$$g_i = \sqrt{\left(S^H \psi^{-1} S\right)^{-1}_{i,i} \left(S^H \psi^{-1} S\right)_{i,i}}. \quad (2)$$

GRAPPA prepared elliptical data were subjected to GRAPPA based parallel reconstruction before any of the spectral processing. In conventional GRAPPA technique, interpolation weights for an individual coil j are synthesized by least squares fitting of acquired lines of all the coils to the AC lines of the j^{th} coil in the Fourier domain as given by the following equation,

$$S_j(k_y - m\Delta k_y) = \sum_{l=1}^{L} \sum_{b=0}^{N_b-1} n(j,b,l,m) S_l(k_y - bR\Delta k_y) \quad (3)$$

where $S_j(k_y\text{-}m\Delta k_y)$ is the signal in the j^{th} coil at $k_y\text{-}m\Delta k_y$ position of *k*-space, b is the number of blocks used for the reconstruction, L is the number of coil elements, and n(j, b, l, m) is the weighting of $S_l(k_y\text{-}bR\Delta k_y)$ for synthesis of S_j ($k_y\text{-}m\Delta k_y$) [6]. For our case, a multi-column multi line interpolation (MCMLI) [7] that used the nearest neighboring points of the time axis (FID) was implemented. The GRAPPA reconstructed data were then processed identically as the full data for spectral processing.

Choline, creatine, and NAA heights were estimated in the frequency domain from the real spectra [4]. Lipid peaks often had a different phase than the other peaks if they were a result of aliasing. NAA, and lipid heights were also separately estimated from the absolute spectra, and lipid contaminated voxels were detected as the ones that had abs(Lip)>abs(NAA) within the Normal regions for the volunteer and patient data. Signal to noise ratio (SNR) was estimated as the height of a peak divided by the standard deviation of the noise calculated from the right hand end of the spectra. Median Cho/NAA ratios were estimated in the normal and tumor regions. A Spearman rank correlation coefficient was used to detect if Cho/NAA results were correlated between the original elliptical data, and SENSE or GRAPPA reduced elliptical data. P values of less than 0.05 were considered significant.

III. RESULTS

Table 1 lists the SNR values of the three metabolites of interest, Cho, Cr, and NAA and table 2 lists the ratio of the SNR values of the metabolites between the original and grappa (O/G), original and SENSE (O/S), and GRAPPA and SENSE (G/S) datasets. SNR is directly proportional to the square root of the data acquisition time. According to the

theoretical estimates, the fully sampled elliptical spectra should have had 1.28 (√952/√582) times more SNR than the GRAPPA elliptical spectra, and 2 (√952/√582) times more SNR than the SENSE elliptical spectra. The theoretical expectation was roughly met for the GRAPPA elliptical spectra. SENSE spectra had almost had one third of the original elliptical SNR which was around 1.5 times less than the expected value. This loss of SNR was due to the noise amplification as a result of the geometry factor effect. Median of the g factors was calculated as 1.57±0.15 for the volunteer, and 1.69±0.34 for the phantom data. Median of the median g factors for the patients was 1.65±0.05.

TABLE 1.

SNR values of the spectral metabolites for the original, GRAPPA, and SENSE elliptical datasets for the patients (median±std)

	ORIGINAL	GRAPPA	SENSE
Cho	38.43±6.14	28.2±5.92	12.55±2.27
Cr	33.38±8.37	25.6±7.16	10.23±2.96
NAA	59.26±15.47	48.26±13.44	19.06±5.46

TABLE 2.

SNR ratios of the metabolites calculated from the original (O), SENSE (S), and GRAPPA (G) median±std elliptical spectra for the patients (median±std)

	O/G	O/S	G/S
Cho	1.33±0.13	3.02±0.25	2.37±0.11
Cr	1.37±0.14	2.98±0.25	2.30±0.11
NAA	1.30±0.13	2.92±0.20	2.31±0.07

Table 3 shows the total number of lipid contaminated voxels for the original, SENSE, and GRAPPA elliptical spectra. It was observed that both GRAPPA and SENSE reconstructions increased the amount of lipid within the normal regions of the spectra. But, this effect was more pronounced for the SENSE reconstruction.

TABLE 3.

Number of voxels that have an absolute lipid height bigger than the absolute NAA height for the three different data types in the normal regions

	ORIGINAL	GRAPPA	SENSE
Volunteer	0	0	5
Patient1	6	23	61
Patient2	0	0	11
Patient3	0	0	5
Patient4	29	50	69
Patient5	1	29	51

Table 4 shows the median Cho/NAA within the tumor and normal regions. It was observed that SENSE and GRAPPA results were similar to the original data results for all the cases. All the patients except patient 2 had increased Cho/NAA levels within the tumor region in comparison to the normal regions.

TABLE 4.

Median Cho/NAA values within the normal and tumor regions for patients, and within the whole PRESS box for the volunteer and phantom data as calculated from the original (O), GRAPPA (G), and SENSE (S) spectra

	NORMAL			TUMOR		
	O	G	S	O	G	S
Volunteer	0.48	0.48	0.49	-	-	-
Phantom	0.56	0.57	0.56	-	-	-
Patient1	0.73	0.74	0.69	1.71	1.64	1.69
Patient2	0.62	0.6	0.6	0.63	0.61	0.60
Patient3	0.62	0.64	0.58	1.45	1.09	1.23
Patient4	0.84	0.83	0.82	2.54	1.52	1.72
Patient5	0.53	0.54	0.53	1.25	0.75	0.78

Spearman rank correlation coefficient results showed a significant ($p<0.05$) correlation of the Cho/NAA ratios between the original and SENSE, and original and GRAPPA elliptical spectra for all the cases within normal regions, and for most of the cases within the tumor regions. Table 5 shows all the rank correlation coefficients (r) within normal and tumor regions. Cho/NAA ratio was not found significantly correlated between GRAPPA and original spectra for patient 4, and it was not significant between SENSE and original spectra for patient 5.

TABLE 5.

Spearman rank correlation coefficient values (r) for the Cho/NAA ratio correlation in the normal and tumor regions between original and grappa (O & G), and original and sense (O & S) spectral results (*: $p<0.05$)

	NORMAL		TUMOR	
	O & G	O & S	O & G	O & S
Volunteer	0.84*	0.85*	-	-
Phantom	0.4*	0.57*	-	-
Patient1	0.63*	0.68*	0.84*	0.82*
Patient2	0.67*	0.72*	0.66*	0.52*
Patient3	0.69*	0.66*	0.69*	0.8*
Patient4	0.45*	0.44*	0.11, p=0.6	0.5*
Patient5	0.66*	0.73*	0.75*	0.26, p=0.11

Figure 2 shows a slice from the phantom data. T1w SPGR image with the spectral PRESS box and spectral selection is shown along with the three different spectra estimates. It was observed that both techniques resulted in spectra that were similar to the original dataset. GRAPPA had some signal variation across the voxels, and SENSE had some voxels that are not fully unaliased like the top right corner voxel.

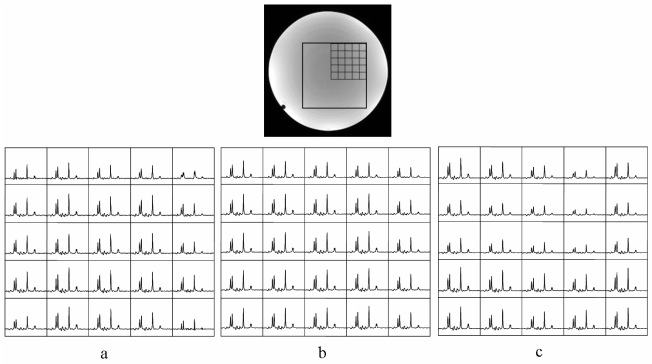

Fig. 2. T1w SPGR image of the phantom is shown at the top row. a. SENSE, b. Original, and c. GRAPPA elliptical spectra.

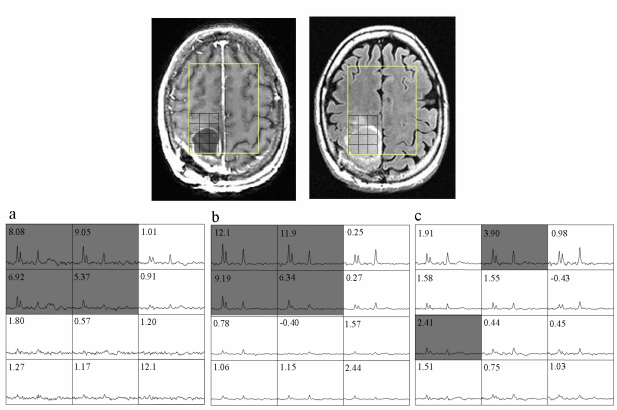

Fig. 3. Top left: T1w SPGR image, and top left: T2w FLAIR image along with the PRESS box (yellow), and some spectral voxels (black box) for a glioma patient. Spectra from the black box is shown at the bottom row as it was estimated by the SENSE (a) ,original (b), and GRAPPA (c) elliptical datasets.

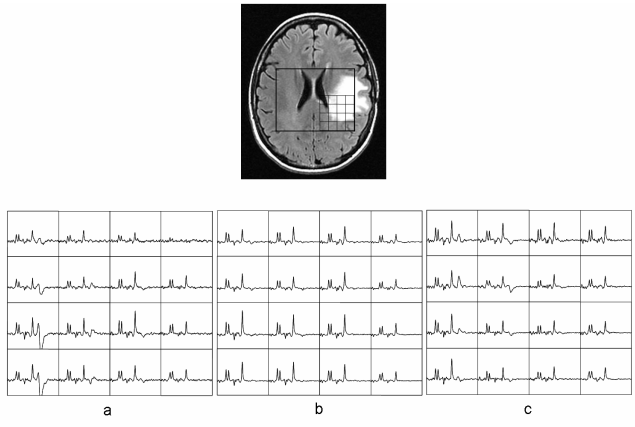

Fig. 4. Top: T2w FLAIR image with the PRESS box, and the selected voxels. Spectra from the black grid is shown as it was estimated by SENSE (a), original (b), and GRAPPA (c) elliptical spectra.

Figure 3 shows an example patient case. T1w SPGR post Gd, and T2w FLAIR images are shown at the top left and right respectively. The PRESS box is shown with yellow, and the spectra from the black box is shown at the bottom row as calculated from the SENSE(a), original (b) and GRAPPA (c) elliptical data. The voxels marked with gray are the ones that had a CNI [2] value bigger than 2, which are typically considered to be tumor voxels. Both spectra showed higher Cho and lower NAA intensities for tumor areas as for the original spectra. GRAPPA intensities were lower at the edge of the cavity, and SENSE had a closer approximation of the tumor areas than GRAPPA in this case. Figure 4 shows another patient example. The spectra estimated from the SENSE elliptical method has been observed to have more residual lipid peaks on the left side of the spectral grid than the GRAPPA method.

IV. DISCUSSION AND CONCLUSION

This study investigated the feasibility of using GRAPPA or SENSE parallel imaging approaches to reduce the MRSI scan time. The techniques were implemented on the elliptically reduced k-space datasets of phantom, volunteer, and patients. Our results showed that both GRAPPA and SENSE elliptical spectra Cho/NAA ratio results had significant correlation with the original elliptical spectra results. An increased lipid artifact was observed in the SENSE elliptical data, due to imperfect unaliasing. GRAPPA elliptical spectra had more intensity variation across the slices than the SENSE spectra, and it resulted in lower intensities around the cavities for tumors. Both spectra would reduce the MRSI scan time significantly, and therefore alleviate the patient discomfort. Further studies will investigate the reasons of GRAPPA intensity variations, and methods of reducing residual lipid artifact for SENSE. GRAPPA technique could be made even more time-efficient by dispensing the need of autocalibration lines using the shift property of the GRAPPA operator.

REFERENCES

[1] American Cancer Society. (March, 2006) Key Statistics for Brain and Spinal Cord Tumors in Adults. Available:http://www.cancer.org/docroot/CRI/content/CRI_2_4_1X_What_are_the_key_statistics_for_brain_and_spinal_cord_tumors_3.asp?sitearea=

[2] S. J. Nelson, "Multivoxel magnetic resonance spectroscopy of brain tumors," *Mol Cancer Ther* , vol. 2, pp. 497-507, May 2003.

[3] X Li , D. B. Vigneron, S. Cha, E. E. Graves, F. Crawford, S. M. Chang, S. J. Nelson, "Relationship of MR-derived lactate, mobile lipids, and relative blood volume for gliomas in vivo," *AJNR Am J Neuroradiol.* vol. 26, pp. 760-9, Apr. 2005.

[4] S. J. Nelson, "Analysis of volume MRI and MR spectroscopic imaging data for the evaluation of patients with brain tumors," *Magn Reson Med,* vol. 46(2), pp. 228-39, Aug. 2001.

[5] U. Dydak, M. Weiger, K. P. Pruessmann, D. Meier, P. Boesiger, "Sensitivity-encoded spectroscopic imaging", *Magn Reson Med,* vol. 46(4), pp. 713-722, Oct. 2001.

[6] M. A. Griswold, P. M. Jakob, R. M. Heidemann, M. Nittka, V. Jellus, J. Wang, B. Kiefer, A. Haase. "Generalized autocalibrating partially parallel acquisitions (GRAPPA)", *Magn Reson Med* vol. 47, pp. 1202-10, Jun 2002

[7] Z. Wang, J. Wang, J. A. Detre, "Improved data reconstruction method for GRAPPA", *Magn Reson Med* vol. 54, pp. 738-42, Sep 2005